

# Supplementary information for “Cultural transmission of move choice in chess”

Egor Lappo<sup>1,†</sup>, Noah A. Rosenberg<sup>1</sup>, and Marcus W. Feldman<sup>1</sup>

<sup>1</sup>Department of Biology, Stanford University, Stanford, CA 94305 USA

<sup>†</sup>Email: [elappo@stanford.edu](mailto:elappo@stanford.edu)

October 10, 2023

## S1 Model fitting

In this section we give details of the fitting procedure and convergence diagnostics for the model of move choice defined in §5(b). For each of the three strategies discussed in §6, the model was fitted using the `cmdstanr` R package, running 4 parallel chains for 10,000 sampling iterations with 2,000 iterations for warm-up. There were no divergent transitions, and reported E-BFMI values were above 0.85 for all chains, showing that the models explored the posterior well (Betancourt 2017; Stan Development Team 2022).

Convergence of the chains was confirmed by visual inspection of traceplots and rank histograms, as well as using the  $\hat{R}$  diagnostic (Gelman and Rubin 1992; Vehtari et al. 2021). The histograms of  $\hat{R}$  values for all  $7k$  model parameters (where  $k$  is the number of strategies) are shown in Figure S1, and all of them are below 1.01, which is considered sufficient evidence for convergence (Stan Development Team 2022).

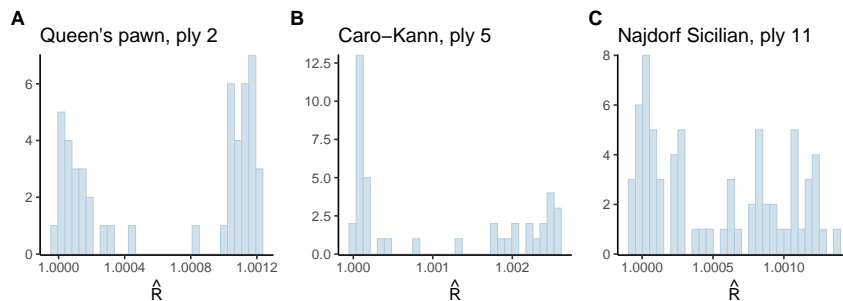


Figure S1: Estimates of  $\hat{R}$  convergence diagnostics for Hamiltonian Monte Carlo model fits. (A) Histogram of the  $\hat{R}$  values for the  $7 \times 7 = 49$  parameters of the Queen’s Pawn opening model. (B) Histogram of the  $\hat{R}$  values for the  $6 \times 7 = 42$  parameters of the Caro-Kann opening model. (C) Histogram of the  $\hat{R}$  values for the  $10 \times 7 = 70$  parameters of the Najdorf Sicilian opening model.

## S2 Model input data

Figure S2 shows the data that was input into the model for each of the three strategies discussed in §6: the raw strategy counts  $x_t^i$ , strategy counts among the top-50 players, strategy win rates in the total population, and win rates among the top-50 players.

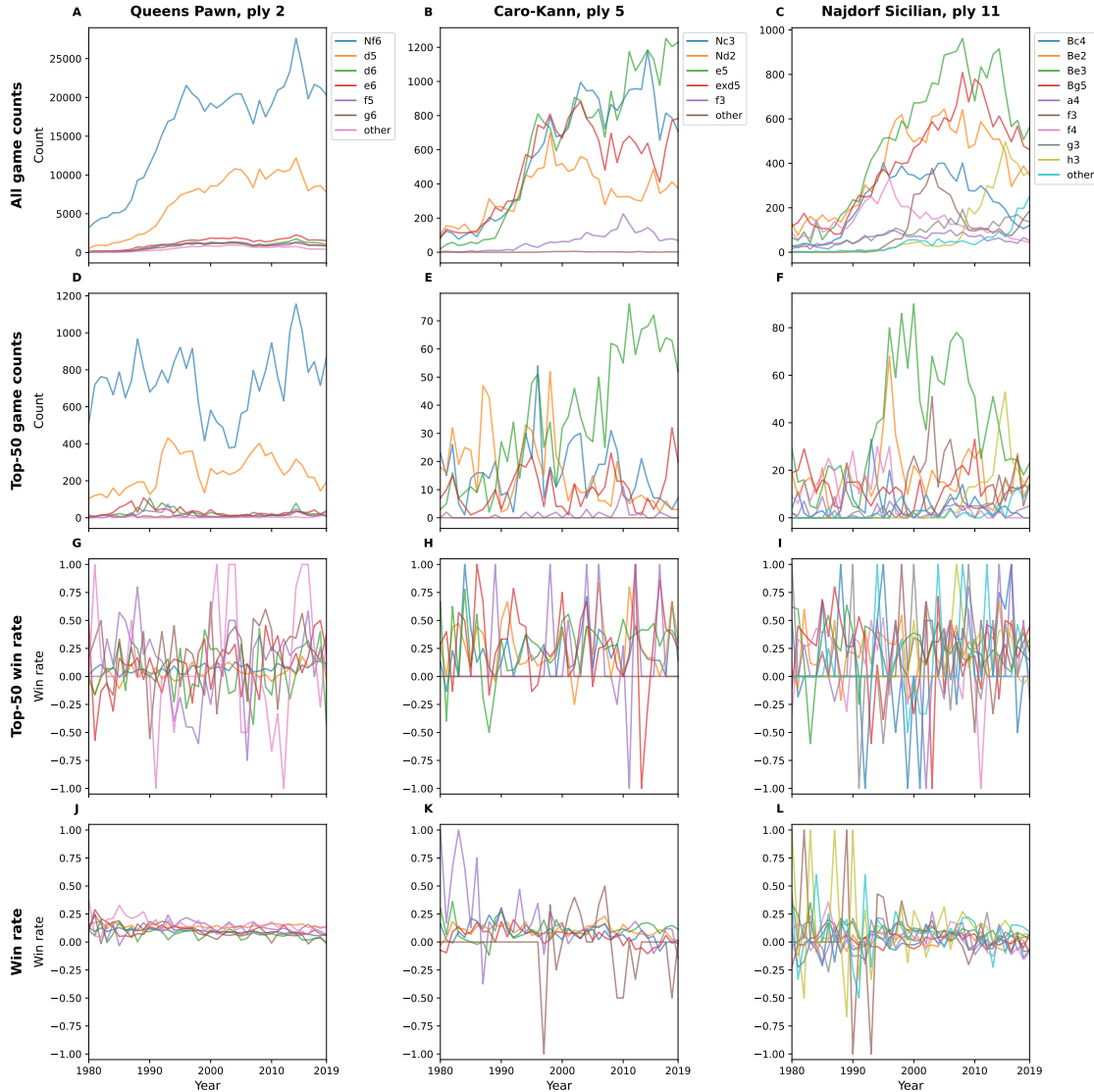


Figure S2: Input data for the Dirichlet-multinomial model for the three positions discussed in §6. (A, B, C) Game counts by strategy for the Queen’s Pawn, Caro-Kann, and Najdorf Sicilian positions respectively. (D, E, F) Counts of games played by the top-50 players for the Queen’s Pawn, Caro-Kann, and Najdorf Sicilian positions, respectively. (G, H, I) Win rates for the Queen’s Pawn, Caro-Kann, and Najdorf Sicilian positions, respectively. (J, K, L) Win rates in games played by the top-50 players for the Queen’s Pawn, Caro-Kann, and Najdorf Sicilian positions, respectively.

## S3 Coefficient estimates

The estimates of the model parameters  $f_i$  and  $\beta_i$  for the three positions discussed in §6 are presented in Figure S3 and Figure S4, respectively.

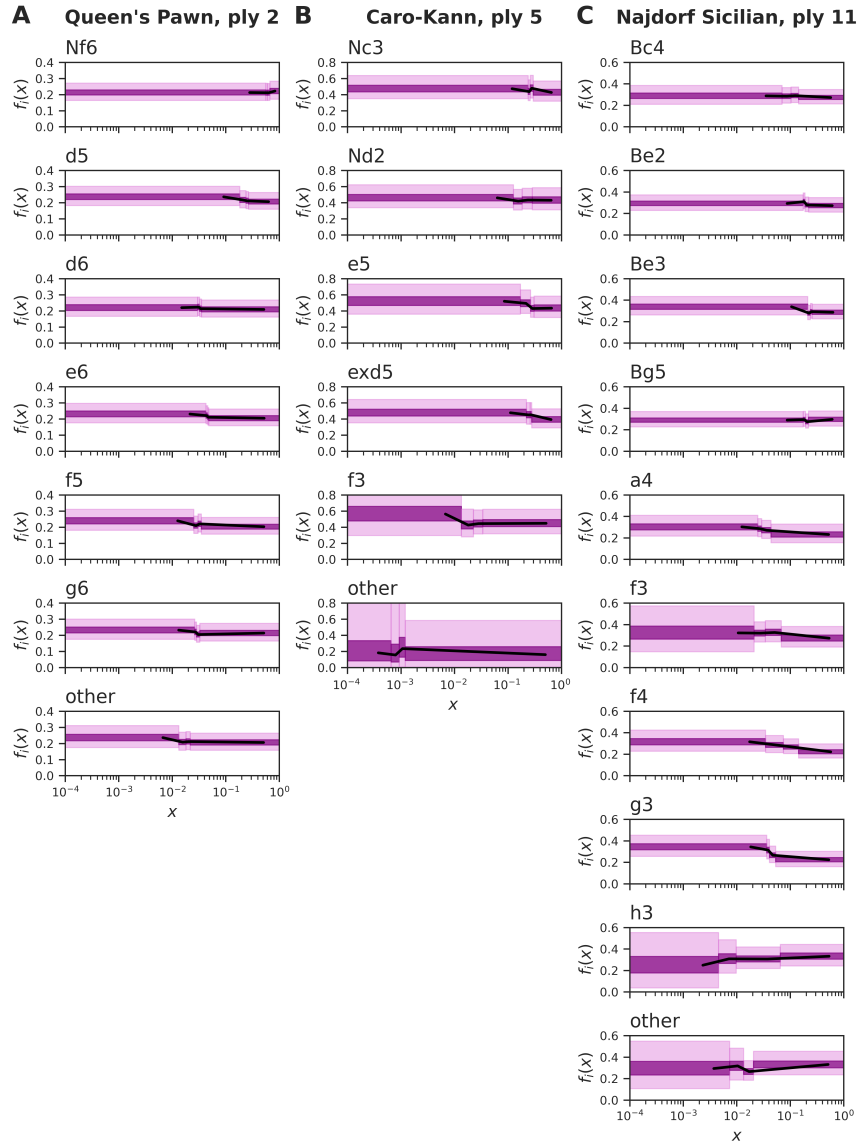


Figure S3: Estimated frequency-dependent fitness functions  $f_i$ . The black line connects the posterior medians for the four constant segments, bright purple shows regions containing 60% of the posterior density, and light purple shows regions containing 98% of the posterior density. (A) Queen's Pawn, ply 2. (B) Caro-Kann, ply 5. (C) Najdorf Sicilian, ply 11.

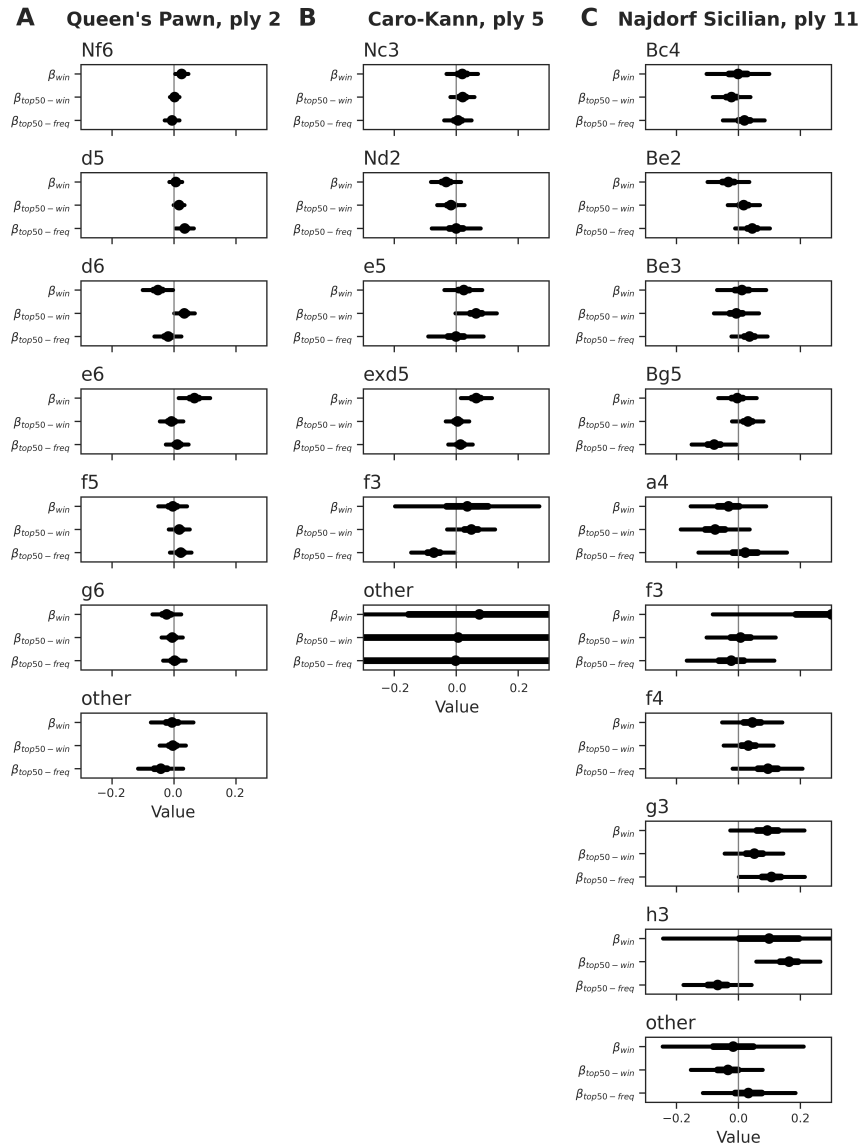


Figure S4: Estimated coefficients  $\beta_i$ . A point marks the posterior median, the thick line marks the region containing 60% of the posterior density, and the thin line shows the region containing 98% of the posterior density. The coefficients presented are:  $\beta_{win}$ , the effect of the average outcome of games in the year previous to that in which a given move was played;  $\beta_{top50-win}$ , the effect of the average outcome of games involving players in the top 50 in the previous year; and  $\beta_{top50-freq}$ , the effect of the frequency of a given move in games involving players in the top 50 in the previous year (see §5(b)). (A) Queen's Pawn, ply 2. (B) Caro-Kann, ply 5. (C) Najdorf Sicilian, ply 11.

## S4 Frequency-dependence characterization

In this section, we describe in detail the procedure used to generate counterfactual predictions for move choice probability in Figure 7. We sample move choice probabilities for year  $t + 1$  from the posterior for our model while keeping as many variables as possible constant in year  $t$ . We fix the number of games at  $N_t = 100,000$  and additionally set the linear features (win rate, win rate among top-50 players, and game count among top-50 players) to be constant and equal to their time averages,

$$\tilde{\mathbf{y}}^i = \frac{1}{40} \sum_{t=0}^{39} \mathbf{y}_t^i.$$

As these linear features were standardized to have zero mean before being input into the model, we must have  $\tilde{\mathbf{y}}^i = 0$  and therefore  $\exp(\boldsymbol{\beta}_i \cdot \tilde{\mathbf{y}}^i) = \exp(0) = 1$  in eq. (20).

Next, for each strategy  $i$ , we generate a sequence of counts  $x_t^i$  from 0 to  $N_t$ . We set the counts of all other strategies to  $x_t^j = (N_t - x_t^i)/(k - 1)$ , where  $i \neq j$  and  $k$  is the number of strategies, which allows for fractional values. This choice of counts keeps the other strategy counts equal while varying the frequency of a strategy of interest.

Finally, we use these input data to sample model predictions of move choice probabilities  $p_t^i$  from the fitted posterior distribution. We first sample coefficients  $c_j^i$  from the posterior, compute coefficients  $\boldsymbol{\alpha}$  using eq. (20), and then sample move probabilities  $p_t$  from  $\text{Dirichlet}(\boldsymbol{\alpha})$ . We repeat this procedure 1,000 times. As a result, for each strategy  $i$  and each initial frequency  $x_t^i$ , we obtain 1,000 samples of move choice probability  $p_t^i$  as estimated by our model. Recall that when strategies are chosen randomly among games in the previous year, the probability of choosing strategy  $i$  is equal to the frequency of  $i$  in the population,  $x_t^i/N_t$ . Comparing our estimates of  $p_t^i$  to  $x_t^i/N_t$ , the expectation under random choice, allows us to characterize frequency-dependent effects in our model.

## S5 Plots of mean fitness $\bar{f}_t$ and game sample size $N_s$

Plots of mean fitness  $\bar{f}_t$  and game sample size  $N_s(t) = N_t \bar{f}_t$  (§6(d)) estimated from the Dirichlet-multinomial model are shown in Figure S5.

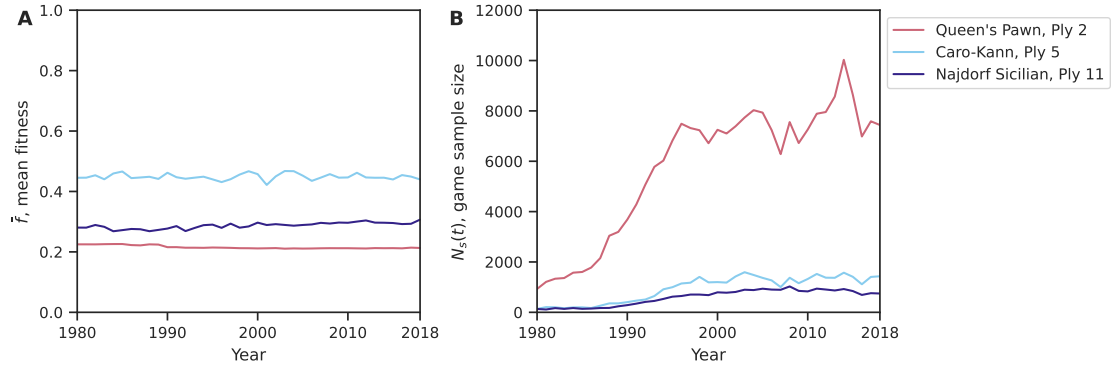


Figure S5: Mean fitness and game sample size estimated by our model for three positions: Queen's Pawn opening, Caro-Kann opening, and Najdorf Sicilian. (A) Mean fitness  $\bar{f}_t$ . (B) Game sample size  $N_s(t) = N_t \bar{f}_t$ .

## References

- Betancourt, Michael (2017). *A conceptual introduction to Hamiltonian Monte Carlo*.
- Gelman, Andrew and Donald B Rubin (1992). “Inference from iterative simulation using multiple sequences”. In: *Statistical Science*, pp. 457–472.
- Stan Development Team (2022). *Runtime warnings and convergence problems*. URL: <https://mc-stan.org/misc/warnings.html> (visited on 07/21/2023).
- Vehtari, Aki et al. (2021). “Rank-Normalization, Folding, and Localization: An Improved  $\hat{R}$  for Assessing Convergence of MCMC (with Discussion)”. In: *Bayesian Analysis* 16.2, pp. 667–718.